Chemical Science

Accepted Manuscript

This article can be cited before page numbers have been issued, to do this please use: Z. Zhou, G. Chen, G. Yu, X. Liu and S. Chou, *Chem. Sci.*, 2026, DOI: 10.1039/D6SC03275C.

ROYAL SOCIETY OF CHEMISTRY

rsc.li/chemical-science

View Article Online
DOI: 10.1039/D6SC03275C

Minireview

Recent Achievements on Nonflammable Electrolytes with Ethoxy(pentafluoro)cyclotriphosphazene for Stable and Safe Lithium-Ion Batteries

Received 00th January 20xx,
Accepted 00th January 20xx

DOI: 10.1039/x0xx00000x

Zhiming Zhou[a,b,c], Guojun Chen[a,b,c], Guojun Yu[a,b,c], Xiaohao Liu[*,a,b,c], Shulei Chou[*,a,b,c]

The increasing demand for high-energy-density lithium-ion batteries (LIBs) has intensified concerns regarding electrolyte flammability, interfacial degradation, and thermal runaway. Phosphazene-based compounds, particularly ethoxy(pentafluoro)cyclotriphosphazene (PFPN), have emerged as promising multifunctional electrolyte compounds that synergistically address these challenges. This review systematically summarizes the molecular design strategies and dual functional mechanisms of phosphazene-based compounds. Their flame-retardant capability operates through gas-phase radical scavenging and condensed-phase barrier effects. P- and N-containing fragments capture H· and OH· radicals to interrupt combustion chain reactions. Simultaneously, these compounds participate in constructing robust, inorganic-rich solid electrolyte interphase and cathode electrolyte interphase films, suppressing electrolyte decomposition and enhancing interfacial stability. The effectiveness of PFPN-based compounds is evaluated across diverse battery systems, including $LiFePO_4$, $LiNi_xCo_yMn_zO_2$, lithium metal, and SiO_x/C anodes, demonstrating significant improvements in cycling stability, overcharge resistance, and thermal safety. Synergistic effects of PFPN with other functional components in composite additive systems are also discussed. Finally, future perspectives are outlined, encompassing advanced in situ characterization, machine learning-assisted electrolyte screening, and validation in large-format cells to accelerate commercial deployment.

1. Introduction

With the rapid advancement of electric vehicles and large-scale renewable energy storage, the demand for lithium-ion batteries (LIBs) that simultaneously deliver high energy density and intrinsic safety has become increasingly urgent.[1-3] However, conventional carbonate-based electrolytes are inherently flammable and thermally unstable, rendering them highly susceptible to thermal runaway under abusive conditions such as overcharge and internal short circuits.[4-6] Although battery management systems can partially mitigate these risks, the intrinsic inconsistency among individual cells within large battery packs, particularly in grid-scale storage, makes it difficult to fundamentally eliminate overcharge-induced hazards. These limitations underscore the pressing need to enhance battery safety at the material level.

To address these challenges, fluorocyclophosphazene compounds have emerged as promising functional components for constructing intrinsically safer electrolytes, owing to their unique structural tunability and multifunctional characteristics. Among them, PFPN stands out as a representative example, having been explored not only as a highly effective flame-retardant additive but also as a co-solvent and functional diluent in advanced electrolyte formulations.[7,8] Whether utilized in trace amounts or as a major component, PFPN provides efficient flame retardancy in the gas phase owing to its high phosphorus content and fluorinated structure. More importantly, its electron-deficient P=N backbone and fluorinated substituents enable the regulation of Li^+ solvation chemistry, promote the formation of robust, inorganic-rich cathode electrolyte interphase (CEI)/solid electrolyte interphase (SEI), and suppress transition-metal dissolution. These versatile roles allow PFPN to effectively address the long-standing trade-off between electrolyte flammability and interfacial instability (Fig. 1)

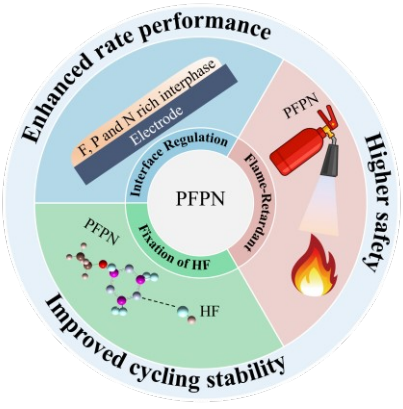

Fig. 1 The role of PFPN in LIBs.

Based on these versatile properties, PFPN has demonstrated irreplaceable application value in various lithium-ion battery systems. This review aims to bridge the gap between intrinsic material characteristics and practical battery performance by systematically summarizing the structure-activity relationships in different cathode

[a] Institute for Carbon Neutralization Technology, College of Chemistry and Materials Engineering, Wenzhou University, Wenzhou, Zhejiang 325035, China. E-mail: liuxh@wzu.edu.cn; chou@wzu.edu.cn
[b] Zhejiang Provincial Key Laboratory of Advanced Battery Materials and Technology, Wenzhou University Technology Innovation Institute for Carbon Neutralization, Wenzhou, Zhejiang 325035, China.
[c] Zhejiang-Australia International Joint Laboratory for Sodium-Ion Batteries, Wenzhou University Technology Innovation Institute for Carbon Neutralization, Wenzhou, Zhejiang 325035, China.

and anode systems. The dual mechanisms of flame retardancy and interfacial regulation are first analyzed, followed by a focused discussion on the practical performance of PFPN in typical battery systems, including lithium iron phosphate (LFP), high-nickel ternary (NCM), lithium metal batteries (LMBs), and SiO_x/C system. By reviewing current research progress, this paper clarifies how PFPN can be employed for precise electrolyte engineering to target the specific issues of different battery systems, such as iron dissolution in LFP and oxidative decomposition in high-nickel cathodes. Finally, the challenges and opportunities for future commercial application are discussed.

2. Role of PFPN

The inherent flammability of conventional electrolytes inevitably poses serious safety threats, including the risk of explosions (Fig. 2a). Therefore, it is urgent to explore intrinsically safe, non-flammable electrolytes that simultaneously boost the safety and electrochemical performance of LIBs. A primary function of PFPN compounds is to enhance the flame retardancy of battery electrolytes, a property that generally originates from both gas-phase radical scavenging and condensed-phase barrier effects. In the gas phase, phosphorus-containing radicals generated during thermal decomposition effectively scavenge highly reactive combustion species, such as H· and O·/OH· radicals, thereby interrupting the radical chain reactions that drive flame propagation (Fig. 2b). In the condensed phase, PFPN decomposes to form a dense, phosphorus-nitrogen-rich char layer, which insulates heat and oxygen, slows volatile release, and suppresses further combustion.

Experimental studies have demonstrated the remarkable flame-retardant efficiency of PFPN.[9-12] For example, incorporating merely 5 vol% PFPN into a conventional carbonate-based electrolyte reduces the self-extinguishing time (SET) from 144.89 to 12.38 $s \cdot g^{-1}$ while increasing the critical oxygen index (COI) from 16.9% to 22.9%, effectively transforming the electrolyte from highly flammable to flame-retardant. Notably, fluorine substitution further enhances flame-retardant performance through synergistic interactions with phosphorus species. Fluorine-derived radicals react with H· radicals to form thermodynamically stable HF, reinforcing radical quenching and chain-termination effects. Additionally, fluorinated substituents improve the compatibility of the additive with electrolyte solvents, alleviating the deterioration of electrochemical performance that is often associated with conventional flame-retardant compounds.[13]

More importantly, the flame-retardant role of PFPN extends beyond its application as a minor additive in conventional electrolyte formulations. When used in large quantities as a co-solvent or functional diluent, the intrinsic nonflammability of PFPN fundamentally reconstructs the solvent environment of the electrolyte, endowing the entire system with inherent flame resistance.[14-18] This design strategy transcends the traditional additive-based approach, which often suffers from a trade-off between flame retardancy and electrochemical performance at high additive loadings.[19] As such, PFPN provides a viable pathway to simultaneously achieve enhanced safety and favorable electrochemical properties.[20,21]

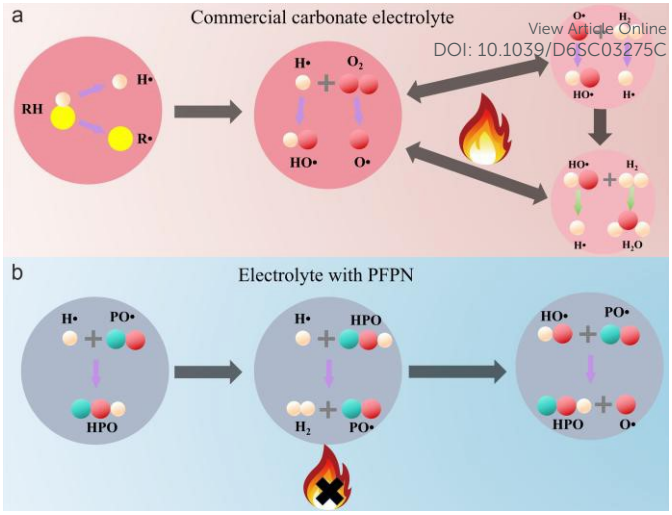

Fig. 2 Schematic of (a) combustion mechanism in commercial carbonate electrolyte and (b) flame retardant mechanism in electrolyte with PFPN.

PFPN compounds can significantly optimize interfacial stability by actively participating in the formation of both the SEI and the CEI.[19]

On the anode side, the P−F and P=N bonds in PFPN molecules are prone to reductive decomposition on the surface of graphite (Gr) or lithium metal.[22,23] These bonds cooperate with the decomposition products of other electrolyte components (e.g., $LiPF_6$) to form an inorganic-rich SEI film abundant in LiF and phosphate species.[24,25] This robust SEI film exhibits high ionic conductivity and structural stability, which inhibits the co-intercalation of solvent molecules, suppresses the growth of lithium dendrites, and thereby reduces charge-transfer impedance. For instance, in LMBs, electrolytes containing PFPN can form an SEI film with a gradient structure, wherein inorganic components (e.g., LiF, Li_2S) are predominantly distributed near the electrode surface, while organic components reside in the outer layer. This unique architecture effectively improves the reversibility of lithium deposition/stripping, maintaining a Coulombic efficiency above 99.2%.

On the cathode side, fluorinated cyclophosphazene compounds mitigate the oxidative decomposition of the electrolyte under high voltage by facilitating the formation of a dense CEI film. For cathode materials such as LFP, LCO, and high-nickel NCM, this CEI film prevents the dissolution of transition-metal ions (e.g., Fe and Ni) and avoids interfacial degradation and short-circuit risks caused by anodic deposition.[26] XPS and TOF-SIMS analyses demonstrate that the CEI film derived from PFPN is rich in P and N species.[27-29] This specific composition inhibits the excessive accumulation of LiF and alleviates HF-induced corrosion of the cathode, thereby enhancing the overall cycling stability of the battery.[30]

3. The application and performance of PFPN

LFP batteries are extensively deployed in large-scale energy storage systems and electric vehicles owing to their superior structural stability and cost-effectiveness. However, potential safety hazards persist, particularly regarding Fe dissolution and electrolyte flammability under overcharge conditions.[31-33] PFPN provides an effective solution to these challenges. In LFP||Gr batteries, the

incorporation of PFPN into the electrolyte does not compromise the cycling stability of the cell, while effectively suppressing the flammability of the electrolyte (Fig. 3a and 3b).[29] When PFPN is added to a baseline electrolyte consisting of 1 M lithium bis(fluorosulfonyl)imide (LiFSI) dissolved in 1,3-dioxolane, it enhances the flame retardancy of the electrolyte and inhibits the corrosion of aluminum foil by the LiFSI salt.[34] The Gr anode delivers reversible capacities of 314.2 mAh g^{-1} and 164.4 mAh g^{-1} at 20 C and 50 C, respectively (Fig. 3c). Furthermore, the LFP||Gr full cell also shows excellent rate performance and cycle performance (Fig. 3d-3f). Moreover, the LFP||Gr full pouch cells maintain a reversible capacity of 127.9 mAh g^{-1} and a high-capacity retention of 99.68% over 500 cycles at 1C (Fig. 3g and 3h).

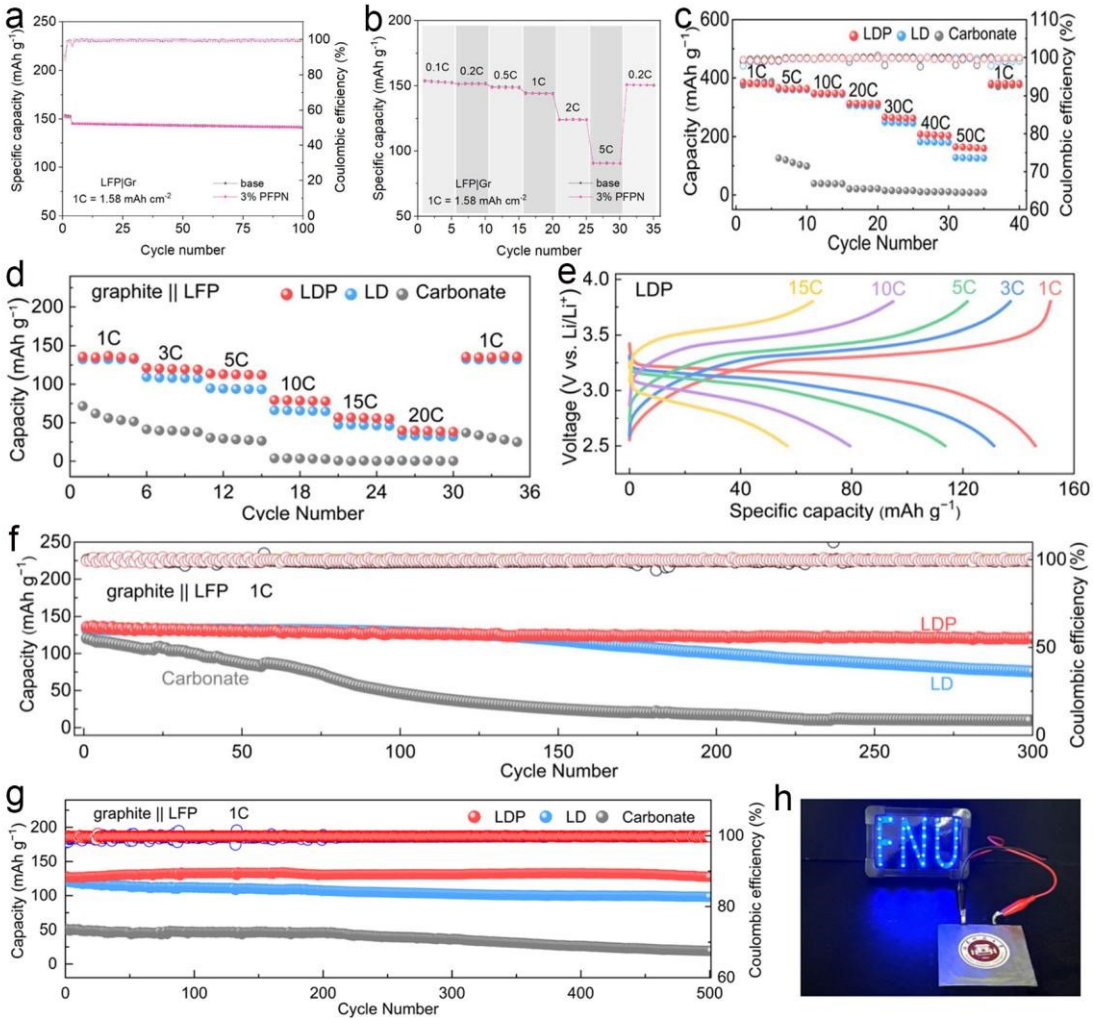

Fig. 3 (a) Long-term cycling performance and (b) rate performance of LFP||Gr full cells. Reproduced with permission.[29] Copyright 2024, The Royal Society of Chemistry. (c) Rate performance of Gr||Li cells. (d) Rate performance, (e) Charge/discharge curves and (f) long-term cycling performance of LFP||Gr full cells. (g) Long-term cycling performance of LFP||Gr pouch cells at 1C. (h) Photograph showing an LED array powered by the LFP||Gr pouch cell. Reproduced with permission.[34] Copyright 2024, The Royal Society of Chemistry.

In practical applications, electrolytes containing PFPN have demonstrated excellent long-term cycling stability in 2 Ah LFP||Gr pouch cells, maintaining a capacity retention of 99.2% after 500 cycles (Fig. 4a).[35] Moreover, under thermal abuse conditions, compared with single-component flame-retardant systems, the composite system combining PFPN with other functional components (e.g., DFEC, HTCN) can delay the occurrence of internal short circuits by nearly 50 minutes (Fig. 4b and 4c), effectively suppress gas evolution (Fig. 4d), and exhibit superior interfacial stability, while maintaining excellent electrochemical performance (Fig. 4e-4g).[36] This approach provides a robust safety guarantee for the application of LFP batteries in large-scale energy storage.

View Article Online
DOI: 10.1039/D6SC03275C

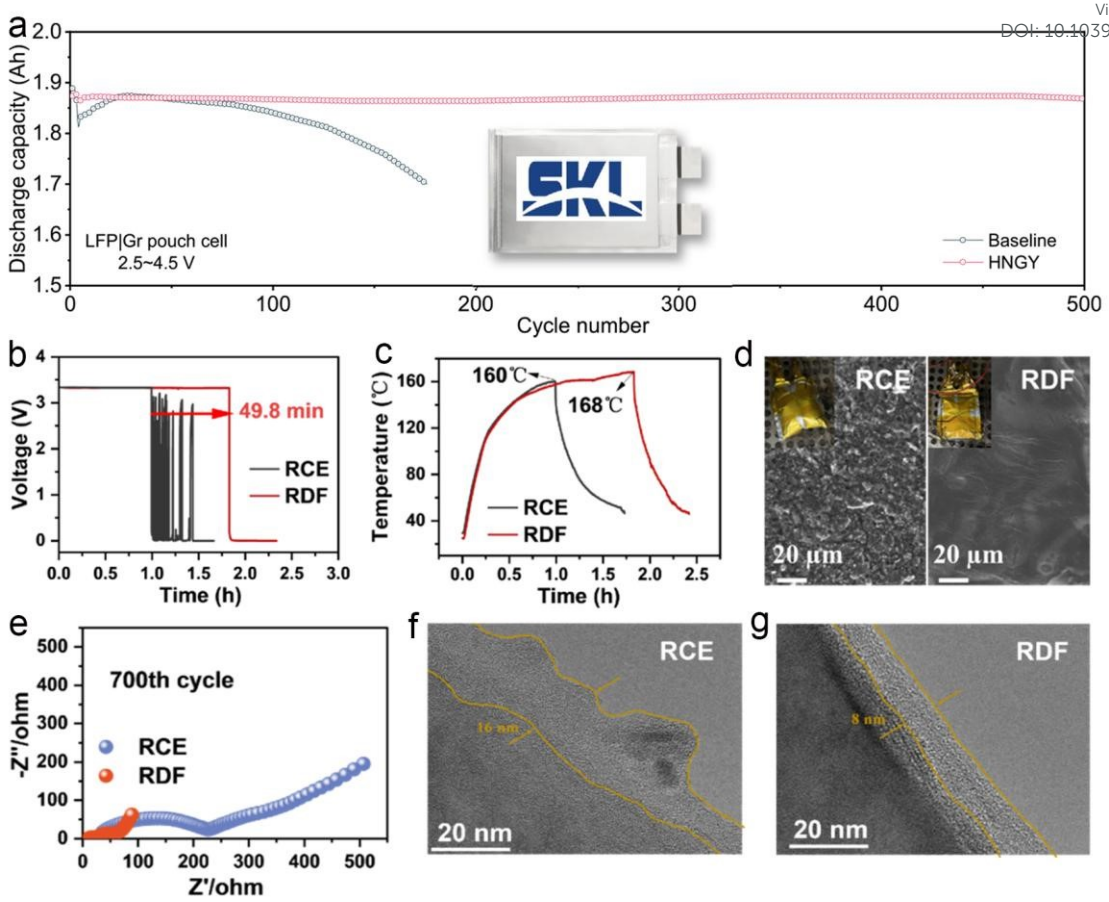

Fig. 4 (a) Electrochemical performance of 2 Ah LFP||Gr pouch cells under 4.5 V overcharge limit. Reproduced with permission.[35] Copyright 2025, Elsevier. (b) Time-voltage profiles of pouch cells filled with RCE and RDF electrolytes during heating in a thermal abuse chamber. (c) Time-temperature profiles of pouch cells filled with RCE and RDF electrolytes during heating in a thermal abuse chamber. (d) SEM images of Gr anodes after thermal abuse for pouch cells along with corresponding optical photographs of the pouch cells. (e) Impedance spectra of Li||Gr half cells at the 700th cycle. (f and g) HRTEM images of graphite anodes after cycling. Reproduced with permission.[36] Copyright 2026, American Chemistry Society.

High-voltage layered cathodes have emerged as the mainstream choice for electric vehicles owing to their high energy density, yet they suffer from severe transition-metal ion dissolution and electrolyte oxidative decomposition under high-voltage operation.[37-42] Concurrently, lithium metal batteries face the dual challenges of lithium dendrite growth and electrolyte flammability. PFPN compounds can significantly enhance the stability of these high-energy-density systems through synergistic interfacial regulation and flame-retardant mechanisms.[25,28]

Upon the introduction of PFPN, the electrolyte undergoes preferential oxidation and decomposition, simultaneously generating linear polymers, polycyclic polymers, $LiNO_3$, $RONO_2Li$ ($RONO_2$: nitrate ester functional group, with R standing for any organic residue), Li_3PO_4, and $ROPO_3Li$ ($ROPO_3$: monoester phosphate) (Fig. 5a). The resulting species form a dense, uniform, and thin protective layer on the surface of the cathode material, which suppresses electrolyte decomposition and electrode corrosion, thereby safeguarding $LiNi_{0.5}Mn_{1.5}O_4$ against structural degradation.[26] In addition, the results of NMR and pH reveal that during cycling, PFPN retains its molecular structure in FEC-based electrolytes while enhancing SEI/CEI stability by acting as a scavenger for the Lewis acidic PF_5 and HF, thereby significantly suppressing the continuous decomposition of FEC and the $LiPF_6$ salt (Fig. 5b-5f).[24]

View Article Online
DOI: 10.1039/D6SC03275C

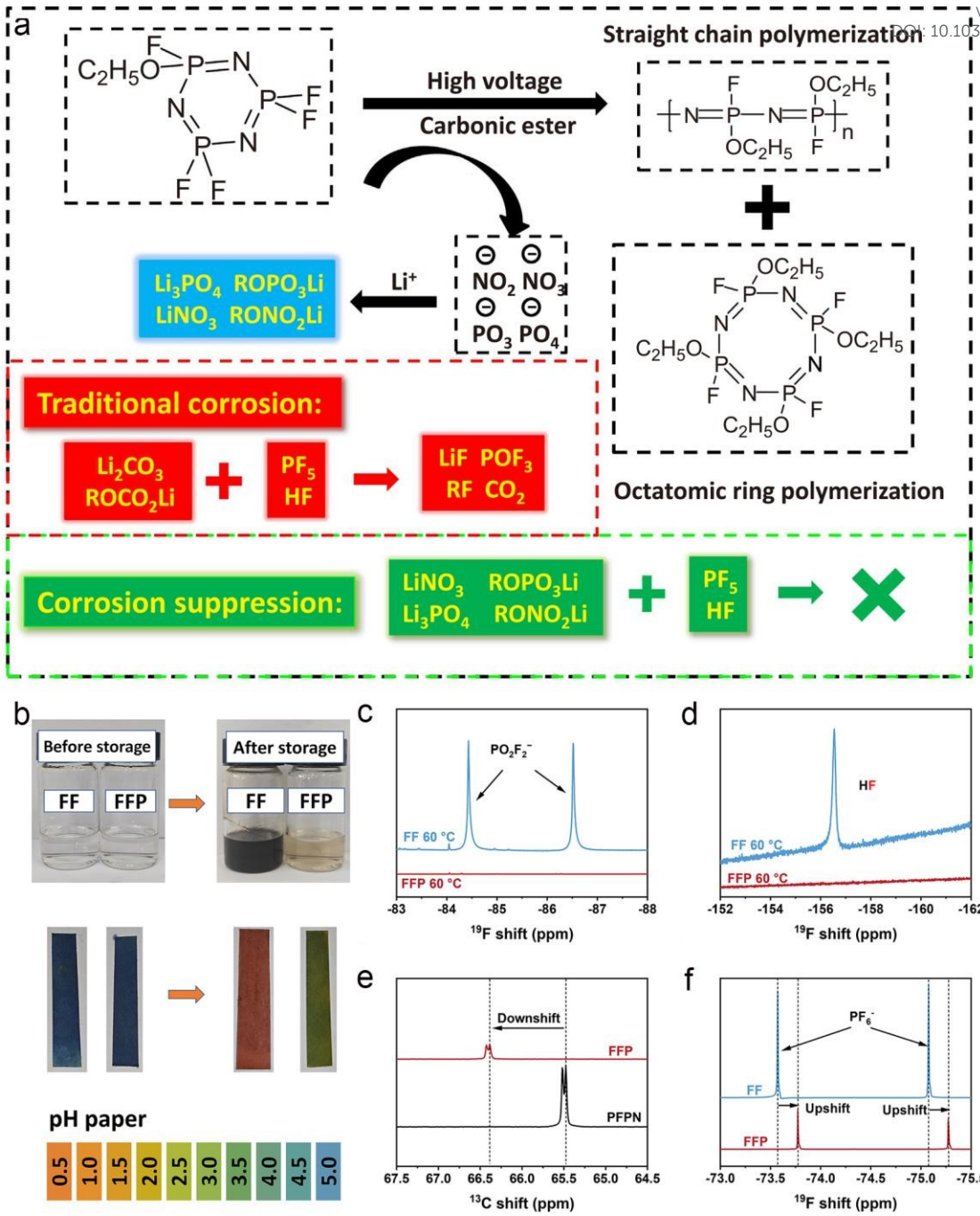

Fig. 5 (a) Illustration of the mechanism of PFPN additive decomposition on the surface of the electrode. Reproduced with permission.[26] Copyright 2018, Elsevier. (b) Photographs and pH of FF and FFP before and after storage at 60 °C for 48 h. (c and d) ^{19}F NMR spectra of FF and FFP after storage at 60 °C for 48 h. (e) ^{13}C NMR spectra of FFP and PFPN. (f) ^{19}F NMR spectra. Reproduced with permission.[24] Copyright 2025, Elsevier.

Furthermore, ultrasonic imaging reveals that the PFPN-containing electrolyte exhibits significantly better wettability than the baseline electrolyte (Fig. 6a). Consequently, a 3 Ah, 4.4 V Li||NCM811 pouch cell employing an FEC/$LiPF_6$-based electrolyte containing 3 wt% PFPN and 2 wt% LiDFOB exhibits stable cycling over 100 cycles at 0.33 C charge and 0.5 C discharge, with excellent capacity retention (Fig. 6b).[30] In thermal abuse tests, the thermal runaway trigger time of batteries using PFPN-containing electrolytes was delayed by approximately 2 h compared with that of batteries using conventional electrolytes, and the onset temperature of thermal runaway increased by 69 °C (Fig. 6c and 6d).[43] When subjected to nail penetration tests, the 2 Ah pouch cells with PFPN-containing electrolytes exhibited no thermal runaway events, such as fire or explosion (Fig. 6e and 6f). $LiNi_{0.8}Mn_{0.1}Co_{0.1}O_2$||Gr pouch cells employing PFPN-containing electrolytes achieved a capacity retention of 94.43% after 600 charge-discharge cycles at 1 C.

View Article Online
DOI: 10.1039/D6SC03275C

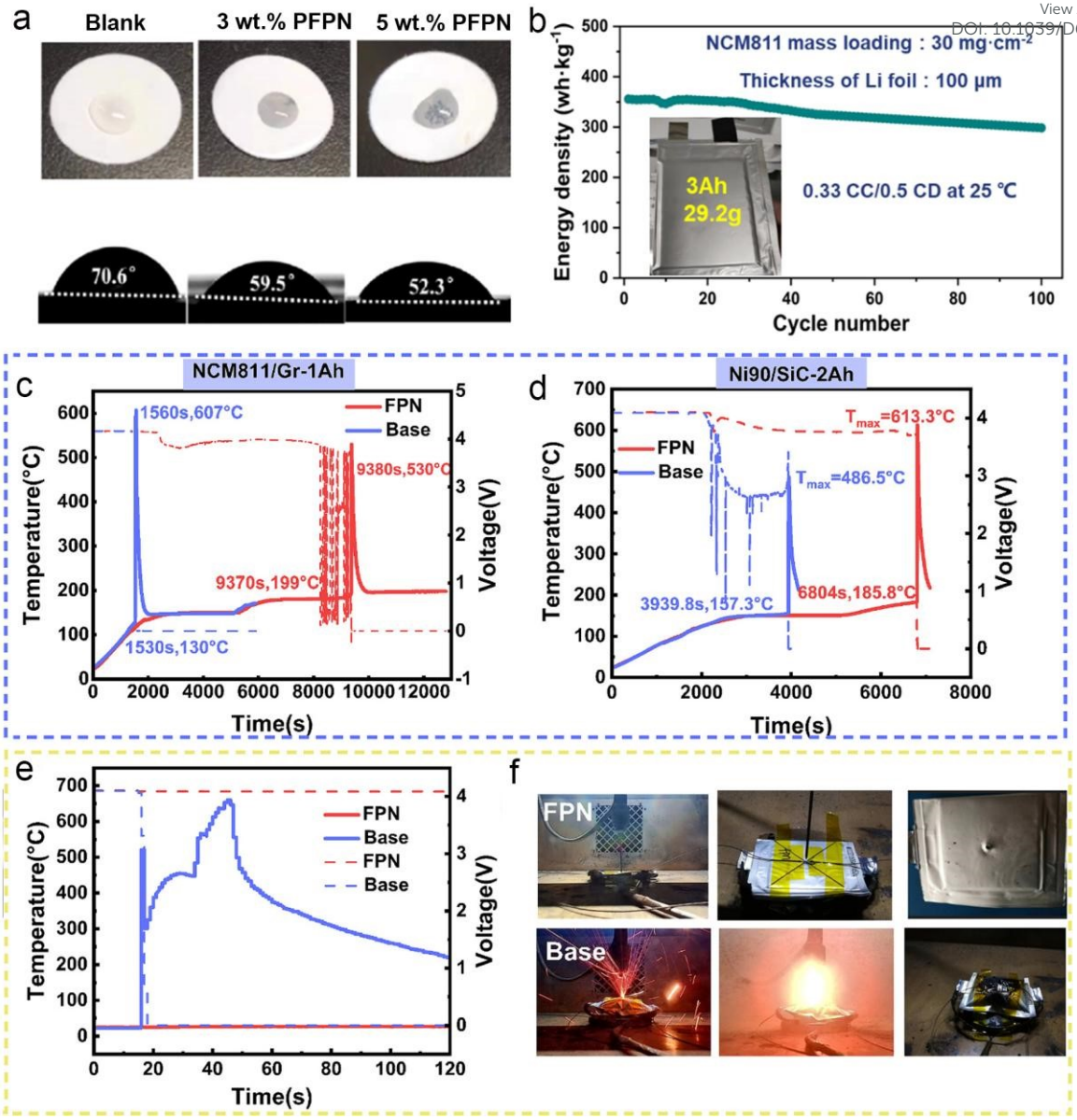

Fig. 6 (a) Wettability and contact angle tests of electrolytes with Celgard 2400 polypropylene (PP) separator. (b) Cycling performance of 3 Ah pouch cell in the optimized electrolyte with electrolyte/capacity of 2.5 g·Ah^{-1}. Reproduced with permission.[30] Copyright 2022, Elsevier. (c) Thermal runaway temperature profiles of SC-NCM811||Gr 1 Ah cells under different electrolytes. (d) Thermal runaway temperature profiles of 2 Ah Ni90||SiC cells under different electrolytes. (e) Temperature profiles during nail penetration test for Ni90||SiC cells with FPN electrolyte and conventional electrolyte. (f) Nail penetration test of 2 Ah Ni90||SiC cells. Reproduced with permission.[43] Copyright 2024, Elsevier.

Particularly in localized high-concentration electrolyte (LHCE) systems, PFPN plays a pivotal role as a functional diluent. While traditional high-concentration electrolytes exhibit excellent performance, they are often limited by high costs and excessive viscosity. Acting as a functional diluent, PFPN effectively reduces both the cost and viscosity of the electrolyte without disrupting the unique solvation sheath structure that is responsible for superior interfacial properties. Simultaneously, it actively participates in interfacial film formation and provides essential flame-retardant protection. With the combination of a carbonate-ether mixture solvent and PFPN as a diluent, the NCM811||Gr cells employing E-PFPN exhibit outstanding cycling performance, with a capacity retention of 82.0% after 1000 cycles at 4.5 V (Fig. 7a and 7b) and 89.8% after 300 cycles at 4.6 V (Fig. 7c).[16] Moreover, the cells also achieve superior cycling stability at elevated temperature (50 °C), retaining 82% capacity after 250 cycles at 4.5 V (Fig. 7d). When PFPN is used as a diluent in a methyl acetate (MA)-based electrolyte, it synergizes with anions to form a protective LiF-rich SEI, which effectively prevents continuous solvent decomposition (Fig. 7e).[15] It enables $LiNi_{0.65}Co_{0.15}Mn_{0.2}O_2$ (NCM65)||Gr full cell to maintain 94.6 % capacity retention after 300 cycles at 1 C and −20 °C (Fig. 7f). Moreover, it allows NCM65||Gr full cell to operate at a high voltage of 4.6 V and −60 °C (Fig. 7g).

View Article Online
DOI: 10.1039/D6SC03275C

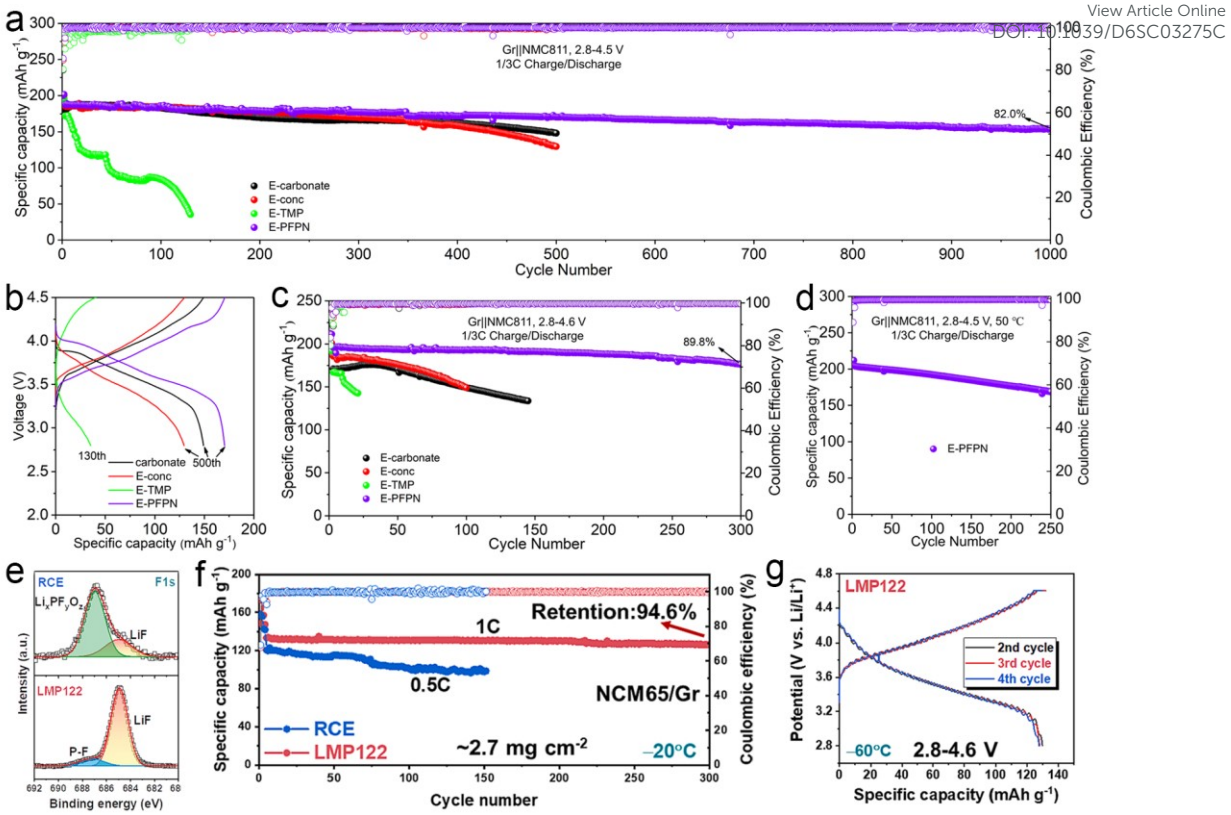

Fig. 7 (a) Cycling stabilities and (b) charge-discharge curves of NCM811||Gr cells at a cut-off voltage of 4.5 V. (c) Cycling stabilities at a cut-off voltage of 4.6 V. (d) Cycling stabilities with 1/3C rate at 50 °C at a cut-off voltage of 4.5 V. Reproduced with permission.[16] Copyright 2023, The Royal Society of Chemistry. (e) F 1s spectra of cycled Gr anodes. (f) Cycling performance of NCM65||Gr cells at −20 °C with potential range from 2.8 to 4.5 V. (g) Charge-discharge curves of NCM65||Gr full cell at −60 °C at a potential range of 2.8-4.6 V. Reproduced with permission.[15] Copyright 2023, Elsevier.

When PFPN, trioxane, and triethyl phosphate (TEP) are mixed, an SEI is formed that exhibits an outer layer of interwoven trioxane-derived polymers and N/P/F-rich inorganic species, along with a deeper region enriched with LiF (Fig. 8a).[23] This SEI inhibits unwanted TEP decomposition at the anode, enabling NCM811||Li full cells to cycle steadily at up to 4.5 V, with an outstanding capacity retention of 92% after 300 cycles (Fig. 8b). In addition, the 1.1 Ah NCM811||Li pouch cells show no signs of thermal runaway upon heating to 250 °C, demonstrating exceptional safety (Fig. 8c). Specifically, the combination of PFPN and ethyl 1,1,2,2-tetrafluoroethyl ether (ETE) enables outstanding performance with $LiNi_{0.5}Co_{0.2}Mn_{0.3}O_2$ (NCM523) cathodes (23.5 mg cm^{-2}). This is attributed to the hydrogen bonding between ETE and DME, along with the coordination of PFPN with Li^+, which weakens the Li^+-DME interaction and promotes an anion-enriched solvation structure (Fig. 8d-8f), thereby facilitating the Li^+ desolvation process and forming an inorganic-rich solid electrolyte interphase.[17] As a result, 80% capacity retention is achieved after 430 cycles at 4.3 V and 84% after 310 cycles at 4.5 V (Fig. 8g), while a 331 mAh pouch cell achieves 148 cycles with 94.9% capacity retention (Fig. 8h).

View Article Online
DOI: 10.1039/D6SC03275C

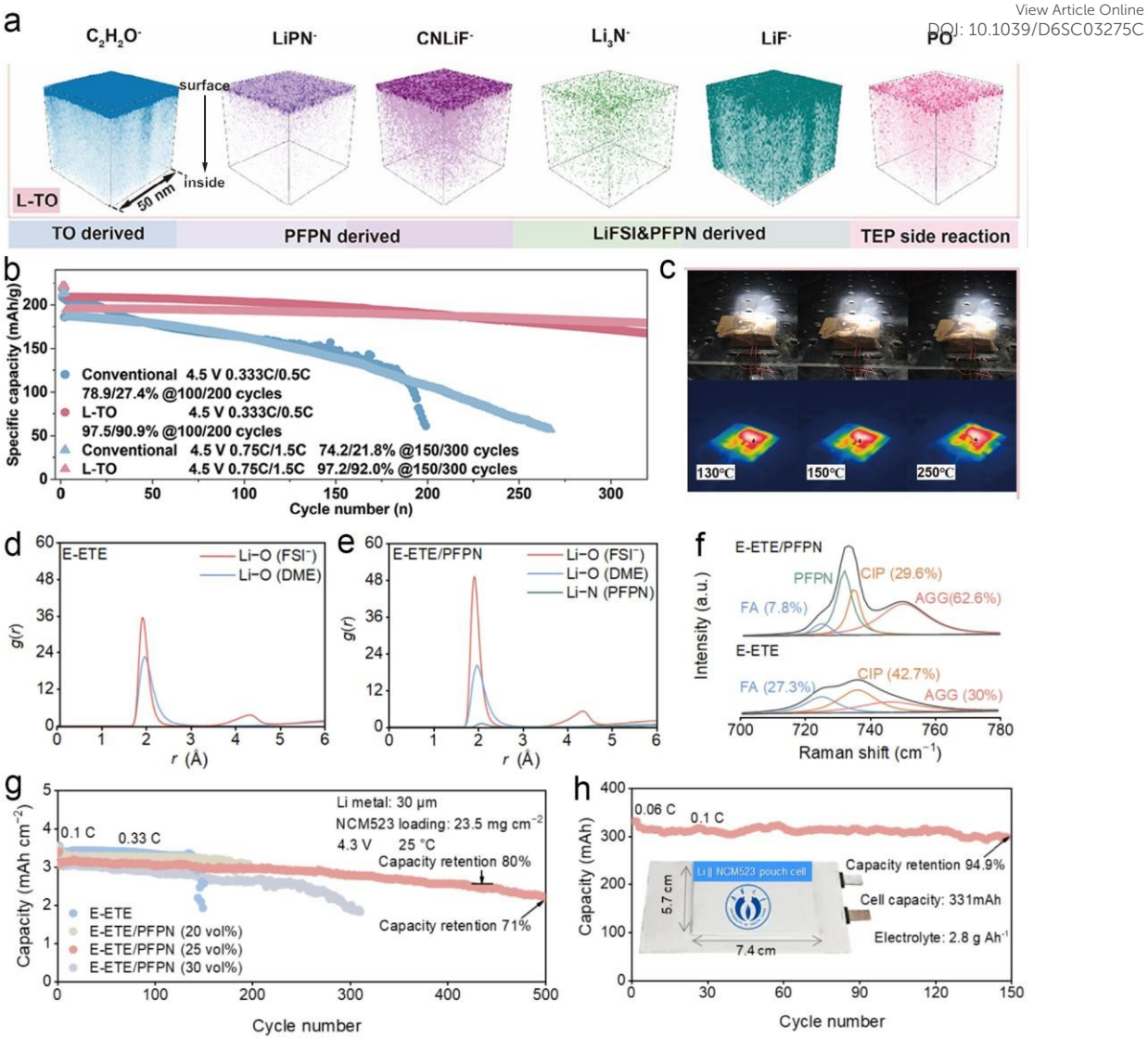

Fig. 8 (a) TOF-SIMS depth profiles of $C_2H_2O^-$, $LiPN^-$, $CNLiF^-$, Li_3N^-, LiF^- and PO^- species on the surface of Li anode after 10 cycles. (b) Cycling stability of NCM811||Li coin cells. (c) Digital photos, and infrared thermographic images for NCM811||Li pouch cells. Reproduced with permission.[23] Copyright 2025, Wiley-VCH. Radial distribution functions calculated from MD simulation of (d) E-ETE and (e) E-ETE/PFPN. (f) Raman spectra. Cycling stability of (g) NCM523||Li coin cells and (h) NCM523||Li pouch cell Reproduced with permission.[17] Copyright 2025, Elsevier.

SiO_x@C anodes are regarded as promising candidates for next-generation lithium-ion batteries owing to their exceptionally high specific capacity. However, their practical application is severely hindered by massive volume expansion during cycling, which causes rupture of the SEI and rapid capacity fading.[44-46] The incorporation of a composite additive system consisting of PFPN and other functional agents provides an effective solution to this challenge. Specifically, the combination of PFPN and FEC facilitates the formation of a dense LiF-rich SEI film. This robust interphase prevents direct contact between the electrolyte and the SiO_x@C anode, thereby mitigating the repeated rupture and reconstruction of the SEI layer. Excellent capacity retention of 87% after 200 cycles at 1 C was achieved for NCM523||SiO_x@C pouch cells with a relatively high SiO_x content of 10% (Fig. 9a).[47] The mechanistic studies further reveal that PFPN cooperates with FEC to induce a unique molecular cling effect (MCE) on SiO_x@C anodes (Fig. 9b). This effect enables PFPN to stably adsorb onto the electrode surface and participate in SEI formation, which cannot be achieved by PFPN alone. Meanwhile, PFPN reacts with key electrolyte intermediates, such as lithium ethyl methyl carbonate (LEMC) and lithium alkoxides, forming thermodynamically stable phosphorus-containing interphase species accompanied by LiF generation. This reaction pathway suppresses the formation of oligomeric hydrocarbon carbonate (OHC) byproducts, reduces parasitic reactions and gas evolution, and lowers cell polarization. As a result, the dual-additive system of FEC and PFPN constructs a uniform, inorganic-rich SEI that accommodates the large volume fluctuations of SiO_x@C during cycling, significantly improving the long-term cycling stability and structural integrity of the electrode (Fig. 9c-9h).

Thermal runaway and safety risks further restrict the application of SiO_x@C anodes, and PFPN-based composite additives can effectively address these issues. PFPN possesses outstanding flame-retardant and

thermal-stabilizing properties: at high temperatures, it decomposes to release fluorine and phosphorus radicals that interrupt combustion chain reactions, enabling self-extinguishing behavior and drastically reducing electrolyte flammability, thereby effectively suppressing thermal runaway and preventing fire/explosion hazards.[48] Recent studies demonstrate that PFPN/tris(2,2,2-trifluoroethyl) borate (TTFEB) significantly enhances thermal stability.[49] the initial exothermic temperature rises from 233.67 to 292.83 °C (Fig. 9i), and the apparent activation energy increases from 439.56 to 1090.01 kJ mol^{-1}, strongly delaying thermal runaway. Meanwhile, this dual-additive system elevates capacity retention from 45.23% to 74.34% over 100 cycles in SiO@C||Li half-cells (Fig. 9j), forms a thinner and more uniform LiF-rich SEI, reduces electrode impedance (Fig.s 9k and 9l), accelerates Li^+ transport, and reinforces electrode structural integrity

Overall, the performance of PFPN-containing electrolytes is highly governed by PFPN molecular features, electrolyte formulation, and battery system chemistry. In conventional graphite- or LFP-based lithium-ion batteries, PFPN mainly acts as a low-dosage flame-retardant and film-forming additive, while inhibiting LiFSI-induced aluminum current collector corrosion. Under thermal abuse conditions, however, single PFPN exhibits limited protection and requires synergistic additives such as DFEC and HTCN for improved safety. For high-voltage layered oxide cathodes, PFPN realizes multifunctional interfacial regulation. It suppresses electrolyte oxidative decomposition and promotes the formation of LiF and phosphate-enriched CEI, which mitigates cathode-electrolyte parasitic reactions and enhances high-voltage stability. In LMBs, PFPN-derived F- and P-containing species build mechanically robust, ion-conductive SEI. Stable interphases still rely on synergistic additives including NaDFOB and FEC. Electrolyte anions also cooperatively regulate interfacial chemistry to construct LiF-rich protective layers. For SiO_x@C anodes, PFPN synergizes with FEC to form dense LiF-rich SEI, alleviating volume-expansion-driven SEI rupture, gas evolution, and side reactions. Nevertheless, PFPN alone cannot stably adsorb on SiO_x@C surfaces or efficiently participate in SEI construction, where the molecular cling effect of FEC is essential. These comparisons highlight that PFPN is not merely a universal flame retardant, but a structure-dependent multifunctional electrolyte component, whose interfacial behavior and high-voltage compatibility are strongly coupled with electrode chemistry and electrolyte design.

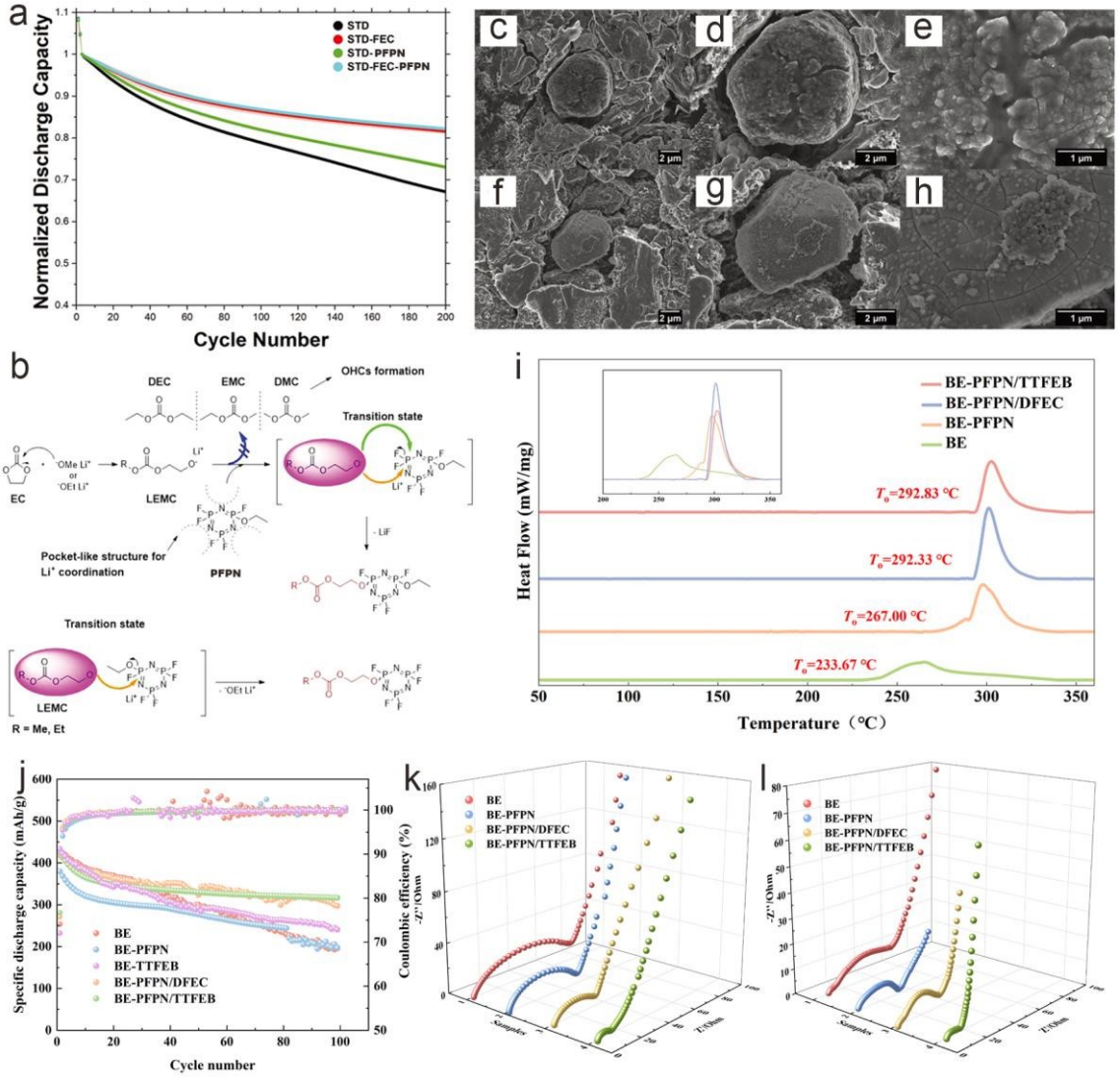

Fig. 9 (a) long-term cycling of NCM523||SiOx@C pouch cells. (b) Proposed reaction mechanism of LEMC with PFPN. SEM images after SEI formation with (c-e) the benchmark STD-FEC electrolyte blend and (f-h) the STD-FEC-PFPN electrolyte blend. Reproduced with permission.[47]

Copyright 2023, Wiley-VCH. (i) DSC curves. (j) long-term cycling of SiO@C||Li cells. EIS results of (k) before cycling and (l) after 100 cycles. Reproduced with permission.[49] Copyright 2024, Elsevier.

View Article Online
DOI: 10.1039/D6SC03275C

4. Conclusions and perspectives

PFPN compounds synergistically enhance the safety and electrochemical performance of lithium-ion batteries through their dual functions of flame retardancy and interfacial regulation. Their flame-retardant mechanism relies on gas-phase effects, while interfacial stabilization is realized through the participation of these compounds in constructing robust SEI and CEI films. Such compounds have exhibited versatile effectiveness across various battery systems, including LFP, NCM, lithium metal, and SiO_x@C anodes, significantly enhancing cycling stability, overcharge resistance, and thermal safety. To better contextualize recent achievements, the electrochemical performance of electrolytes containing PFPN reported in the literature is summarized in Table 1. From an industrial perspective, PFPN is currently commercially accessible as a specialty chemical and can be incorporated into electrolyte formulations using conventional manufacturing processes, suggesting good short-term scalability. Nevertheless, its large-scale deployment will depend on further evaluation of bulk synthesis cost, supply-chain maturity, and compatibility with large-format cell production.

View Article Online
DOI: 10.1039/D6SC03275C

Table 1. Electrochemical performance of the representative electrolytes with PFPN for LIBs.

Formula	Cathode||Anode	Voltage	Discharging rate	Cycling stability (capacity retention/cycles)	Performance in Ah-level pouch cells	SET/thermal runaway trigger temperatures	Ref.
1.0 M $LiPF_6$ in EC:DMC (1:1 by vol) + 3 wt% PFPN	LFP||Gr	2.5-4.0 V	1 C	97.25% 100 cycles	/	lower than 10 s g^{-1}	29
1.0 M LiFSI in DOL:PFPN (9:1 by vol)	LFP||Gr	2.5-3.8 V	1 C	88.7% 300 cycles	/	0 s g^{-1}	34
1.0 M $LiPF_6$ in EC:DMC (3:7 by vol) + 4 wt% D_3F+ 3 wt% FK+ 1.7 wt% PFPN	LFP||Gr	2.5-3.8 V	0.2 C	80.5% 200 cycles	93% 200 cycles (1Ah)	3 s g^{-1}/168 °C	36
1.0 M $LiPF_6$ in EC:DEC:DMC (1:1:1 by vol) + 5 wt% PFPN	$LiNi_{0.5}Mn_{1.5}O_4$|| Gr	2.5-5.0 V	1 C	87.3% 100 cycles	/	0 s g^{-1}	26
1.0 M $LiPF_6$ in EC:DEC (1:1 by vol) + 10 wt% PFPN	$LiNi_{0.5}Mn_{1.5}O_4$|| Gr	3.0-4.9 V	0.5 C	90.7% 100 cycles	/	0 s g^{-1}	25
LiFSI:DME:FEC:PFPN (1:1.5:0.5:3 by mol)	NCM811||Gr	2.8-4.5 V	1/3 C	82.0% 1000 cycles	/	0 s g^{-1}	16
1.5 M LiFSI in DME:PFPN (1:2 by vol)	NCM811||Li	3.0-4.3 V	0.5 C	86.5% 200 cycles	/	0 s g^{-1}	14
1.0 M $LiPF_6$ in EC:DMC:EMC (1:1:1 by vol) + 7 wt% PFPN	NCM811||Li	3.0-4.5 V	1 C	89.5% 200 cycles	/	0 s g^{-1}	28
LiFSI:DMC:PFPN (1:3:3 by mol)	$LiCoO_2$||Li	3.0-4.5 V	2 C	86.0% 1000 cycles	/	0 s g^{-1}	18
0.8 M LiFSI + 0.2 M LiTFSI + 0.6 M $LiPF_6$ in PC:EMC (1:2 by vol) + 6 wt% PFPN	NCM811||Gr	3.0-4.3 V	1 C	94.43% 600 cycles	/	0 s g^{-1}/199 °C	43
1.5 M LiFSI in TEP:PFPN (1:2 by vol) + 1 wt% trioxane	NCM811||Li	2.8-4.5 V	1.5 C	92.0% 300 cycles	/	0 s g^{-1}/250 °C	23
LiFSI:DME:ETE:PFPN (1:1.2:1.6:0.8 by mol)	NCM523||Li	2.8-4.5 V	0.33 C	84.0% 310 cycles	/	0 s g^{-1}	17
1.0 M $LiPF_6$ in EC:DMC:EMC (1:1:1 by wt) + 10 vol% PFPN	NCM811||Gr	2.7-4.5 V	1/3 C	81.7% 200 cycles	83.2% 500 cycles (1Ah)	0 s g^{-1}/168.2 °C	19

To promote the application of PFPN-containing electrolytes in LIBs for stable and safe energy storage, future research should focus on the following aspects: (i) The decomposition pathways of PFPN under realistic electrochemical conditions should be clarified. The P=N backbone, P–F bonds, and ethoxy substituent may undergo reductive or oxidative cleavage, producing LiF-, Li_3N-, and phosphate-rich interphases. However, the exact sequence of bond breaking and its dependence on local Li^+ solvation remain unclear. Advanced in situ/operando spectroscopic techniques, including in situ Raman, nuclear magnetic resonance (NMR), X-ray absorption fine structure (XAFS) spectroscopy, and online gas analysis should be integrated with first-principles calculations and theoretical simulations to identify PFPN-derived intermediates and correlate molecular decomposition with SEI/CEI formation. (ii) the compatibility of PFPN with high-voltage cathodes requires deeper investigation. For NCM811, Ni-rich layered oxides, Li-rich layered oxides, LNMO, and high-voltage LCO, PFPN may simultaneously act as a sacrificial film-forming additive, HF/PF_5 scavenger, and flame

retardant. However, oxidative decomposition, gas generation, transition-metal dissolution, and impedance growth remain potential failure modes. Advanced imaging techniques (e.g., cryo-TEM, in situ AFM, SEM, and TOF-SIMS depth profiling) should be applied to track the evolution of PFPN-derived CEI layers during long-term high-voltage cycling. (iii) Future molecular design should strike a balance among flame retardancy, viscosity, ionic conductivity, high-voltage stability and gas evolution. Compared with other phosphazene derivatives and conventional flame retardants, PFPN delivers superior flame-retardant efficiency and interfacial protection, yet suffers from high cost, limited solubility, and compromised electrochemical performance at high dosages, with P-F/P-O-C bond cleavage-induced gas evolution as its main failure mode. Increasing PFPN content generally improves flame-retardant performance yet impairs battery electrochemical properties; moreover, the cleavage of P-F or P-O-C bonds under harsh conditions generates gaseous by-products. Machine learning models trained on molecular descriptors, including HOMO/LUMO energy levels, bond dissociation energy, solvation free energy, oxidation/reduction potential, viscosity, conductivity, SET, COI and gas generation data, can accelerate the screening of next-generation phosphazene derivatives with balanced performance. (iv) PFPN-containing electrolytes should be validated in practical full cells. Most current studies remain based on coin cells, where heat dissipation and gas accumulation differ from commercial batteries. Future studies should evaluate Ah-level pouch, cylindrical, and prismatic cells under high-voltage cycling, elevated temperature storage, overcharge, nail penetration, and accelerating rate calorimetry conditions. (Fig. 10).

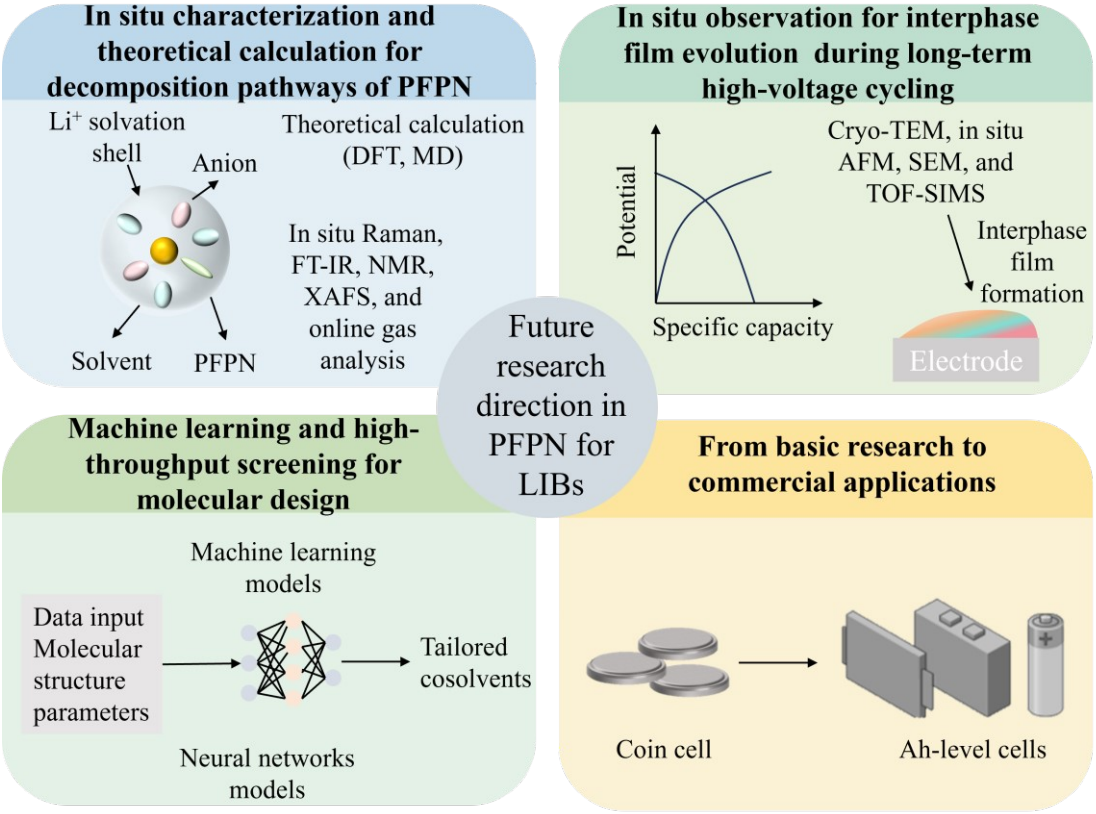

Fig. 10 Four future research direction of electrolyte with PFPN for LIBs.

Data availability

The type of this manuscript is a review and related data are cited from others. Therefore, there are no raw experimental or computational data associated with this article.

Author contributions

Z. Zhou designed the structure of the review. G. Chen and G. Yu collected the papers related to this review topic. X. Liu and S. Chou supervised the review. The manuscript was revised by all the authors.

Conflicts of interest

There are no conflicts to declare.

Acknowledgements

This work was supported by the National Natural Science Foundation of China (52250710680), High-end Foreign Experts Recruitment Plan of China (G2023016009L), Key Research and Development Program of Zhejiang Province (2024C01057, 2023C01232), Central Government Guidance Fund for Local Science and Technology Development (2025ZY01041), Science and Technology Plan Project of Wenzhou Municipality (ZG2022032), Basic Research Project of Wenzhou City (GK20250158).

References

1. Y. Tian, G. Zeng, A. Rutt, T. Shi, H. Kim, J. Wang, J. Koettgen, Y. Sun, B. Ouyang, T. Chen, Z. Lun, Z. Rong, K. Persson and G. Ceder, Promises and Challenges of Next-Generation "Beyond Li-ion" Batteries for Electric Vehicles

and Grid Decarbonization, *Chem. Rev.*, 2021, **121**, 1623-1669.

2. C. Li, J. Liu, Y. Su, J. Dong, H. Zhang, M. Wang, Y. Guan, K. Yan, N. Liu, Y. Lu, N. Li, Y. Su, F. Wu and L. Chen, Enhancing chemomechanical stability and high-rate performance of nickel-rich cathodes for lithium-ion batteries through three-in-one modification, *Energy Storage Mater.*, 2025, **74**, 103893.
3. H. Zhang, J. Dong, Y. Lu, Y. Liu, J. Hao, N. Li, G. Chen, Q. Huang, Y. Su, F. Wu and L. Chen, Molten-salt-mediated crystal facet engineering for high-performance single-crystal nickel-rich cathode materials in lithium-ion batteries, *Nano Energy*, 2025, **142**, 111177.
4. C. M. Grégoire, Y. M. Almarzooq, E. L. Petersen and O. Mathieu, Experimental and modeling study of the combustion of ethyl methyl carbonate, a battery electrolyte, *Combust. Flame*, 2024, **260**, 113225.
5. L. Zhao, J. Hou, X. Feng, J. Xu, C. Xu, H. Wang, H. Liu, B. Hou, X. Rui, Y. Gu, L. Lu, C. Bao and M. Ouyang, The trade-off characteristic between battery thermal runaway and combustion, *Energy Storage Mater.*, 2024, **69**, 103380.
6. B. Mao, H. Chen, L. Jiang, C. Zhao, J. Sun and Q. Wang, Refined study on lithium ion battery combustion in open space and a combustion chamber, *Process Safety and Environmental Protection*, 2020, **139**, 133-146.
7. T. Dagger, B. R. Rad, F. M. Schappacher and M. Winter, Comparative Performance Evaluation of Flame Retardant Additives for Lithium Ion Batteries - I. Safety, Chemical and Electrochemical Stabilities, *Energy Technol.*, 2018, **6**, 2011-2022.
8. Z. Zhou, Y. Qian, Y. Wan, X. Xu, X. Zhang, X. Zeng, X. Zhou, X. Wu, X. Chen, J. Wang, S. Chou and L. Li, Recent achievements on nonflammable triethyl phosphate-based electrolytes for stable and safe lithium metal batteries, *Sci. China Chem.*, 2025, **68**, 5541-5555.
9. W. L. Wang, H. L. Hu, X. Y. Zeng, W. Z. Fan, T. X. Yang, X. Y. Zhao, C. J. Fan, X. X. Zuo and J. M. Nan, Comprehensive Insight into the Probability of Cyclotriphosphazene Derivatives as the Functional Electrolyte Additives in Lithium-Ion Batteries: Which Is Better and Why?, *ACS Appl. Energy Mater.*, 2021, **4**, 7101-7111.
10. A. Yusuf, V. S. Avvaru, J. de la Vega, M. Y. Zhang, J. G. Molleja and D. Y. Wang, Unveiling the structure, chemistry, and formation mechanism of an in-situ phosphazene flame retardant-derived interphase layer in $LiFePO_4$ cathode, *Chem. Eng. J.*, 2023, **455**, 140678.
11. S. Sayah, M. Baazizi, M. Karbak, J. Jacquemin and F. Ghamouss, Deep and Comprehensive Study on the Impact of Different Phosphazene-Based Flame-Retardant Additives on Electrolyte Properties, Performance, and Durability of High-Voltage LMNO-Based Lithium-Ion Batteries, *Energy Technol.*, 2023, **11**, 2201446.
12. C. Clephas, B. Heidrich, M. Winter and P. Niehoff, Low Voltage Formation Process for Lithium Ion Battery Cells, *J. Electrochem. Soc.*, 2025, **172**, 050504.
13. X. Li, W. K. Li, L. Chen, Y. Lu, Y. F. Su, L. Y. Bao, J. Wang, R. J. Chen, S. Chen and F. Wu, Ethoxy (pentafluoro) cyclotriphosphazene (PFPN) as a multi-functional flame retardant electrolyte additive for lithium-ion batteries, *J. Power Sources*, 2018, **378**, 707-716.
14. Q. Q. Liu, Y. Liu, Z. R. Chen, Q. Ma, Y. R. Hong, J. H. Wang, Y. F. Xu, W. Zhao, Z. K. Hu, X. Hong, J. W. Wang, X. L. Fan and H. B. Wu, An Inorganic-Dominate Molecular Diluent Enables Safe Localized High Concentration Electrolyte for High-Voltage Lithium-Metal Batteries, *Adv. Funct. Mater.*, 2023, **33**, 2209725.
15. S. Lei, Z. Q. Zeng, M. C. Liu, M. S. Qin, Y. K. Wu, Y. L. Zhu, S. J. Cheng and J. Xie, Nonflammable cosolvent enables methyl acetate-based electrolyte for 4.6 V-class lithium-ion batteries operating at-60 °C, *Chem. Eng. J.*, 2023, **478**, 147180.
16. L. Chen, Q. S. Nian, D. G. Ruan, J. J. Fan, Y. C. Li, S. Q. Chen, L. J. Tan, X. Luo, Z. Z. Cui, Y. F. Cheng, C. H. Li and X. D. Ren, High-safety and high-efficiency electrolyte design for 4.6 V-class lithium-ion batteries with a non-solvating flame-retardant, *Chem. Sci.*, 2023, **14**, 1184-1193.
17. Y. Wang, Y. Li, C. Z. Li, Y. H. Guo, L. X. Yu, X. Li and T. Li, Weakening Li^+-solvent interaction with dual diluents enabling high-performance lithium metal batteries, *J. Energy Chem.*, 2025, **106**, 681-687.
18. H. Zhang, Z. Q. Zeng, S. P. Wang, Y. K. Wu, C. H. Li, M. C. Liu, X. L. Wang, S. J. Cheng and J. Xie, High-safety and high-voltage lithium metal batteries enabled by nonflammable diluted highly concentrated electrolyte, *Nano Res.*, 2024, **17**, 2638-2645.
19. W. F. Zhang, X. N. Feng, W. S. Huang, L. G. Lu, H. W. Wang, L. Wang, X. M. He, M. D. Wei and M. G. Ouyang, Thermal Runaway Inhibition of Lithium-Ion Batteries Employing Thermal-Driven Phosphazene Based Electrolytes, *Adv. Funct. Mater.*, 2025, **35**, 2508688.
20. C. Y. Wang, Y. Xiao, G. Z. Chen, L. M. Bai, T. J. Fu, X. Ma, Z. Q. Jin, X. B. Hong, J. T. Zuo and D. Z. Li, Nonflammable localized high-concentration electrolytes with 1,3-dioxolane coordination regulation, *Chem. Eng. J.*, 2025, **525**, 170477.
21. X. J. Li, Y. T. Wang, X. X. Yan, Y. C. Liu, W. S. Jia, L. X. Feng, X. P. Zhang and T. Chen, Interaction strength of phosphorus co-solvents in 1,3-dioxolane based electrolytes governs flame retardancy and cycling stability of lithium-metal batteries, *J. Colloid Interface Sci.*, 2026, **707**, 139651.
22. W. Zhong, R. J. He, L. F. Peng, W. Liu, J. Y. Peng, H. L. Zhu, J. Y. Xiang, S. J. Cheng and J. Xie, Lifecycle Synergistic Prelithiation Strategy of Both Anode and Cathode for High-Performance Lithium-Ion Batteries, *Adv. Energy Mater.*, 2025, **15**, 2406007.
23. Z. Y. Gao, Q. Y. Tan, L. Zhu, J. B. Dan, L. B. Tang, J. J. Li, N. Hussain, X. Gao, X. C. Lou, X. Y. Zhang, S. J. Luo, L. N. Zhou, L. Zhong, B. Q. Chen and T. Liu, A Fully Flame-Retardant Electrolyte with Laminated SEI for Exceptionally Safe, Long-Life, and High-Voltage Lithium Metal Batteries, *Small*, 2025, **21**, 2500971.
24. M. S. Li, L. S. Xu, A. Q. He, H. J. Xie and K. R. Deng, Self-cleaning all-fluorinated nonflammable electrolyte for high-voltage and high-temperature Li||NCM811 batteries, *Energy Storage Mater.*, 2025, **77**, 104208.
25. Q. Q. Liu, Z. R. Chen, Y. Liu, Y. R. Hong, W. N. Wang, J. H. Wang, B. Zhao, Y. F. Xu, J. W. Wang, X. L. Fan, L. S. Li and H. B. Wu, Cooperative stabilization of bi-electrodes with robust interphases for high-voltage lithium-metal batteries, *Energy Storage Mater.*, 2021, **37**, 521-529.
26. J. W. Liu, X. Song, L. Zhou, S. Q. Wang, W. Song, W. Liu, H. L. Long, L. X. Zhou, H. M. Wu, C. Q. Feng and Z. P. Guo, Fluorinated phosphazene derivative - A promising electrolyte additive for high voltage lithium ion batteries: From electrochemical performance to corrosion mechanism, *Nano Energy*, 2018, **46**, 404-414.
27. S. F. Liu, M. Becker, Y. Huang-Joos, H. G. Lai, G. Homann, R. Grissa, K. Egorov, F. Fu, C. Battaglia and R. S. Kuehnel, Multifunctional Additive Ethoxy(pentafluoro)cyclotriphosphazene Enables Safe

Carbonate Electrolyte for SiO_x-Graphite/NMC811 Batteries, *Batteries Supercaps*, 2023, **6**, e202300220.

28. Y. D. Zhang, P. Wei, B. Zhou, H. S. Zhao, Z. H. Wang, J. M. Ma and Y. R. Ren, Multifunctional Electrolyte Additive for High-Nickel $LiNi_{0.8}Co_{0.1}Mn_{0.1}O_2$ Cathodes of Lithium-Metal Batteries, *Energy & Fuels*, 2023, **37**, 11388-11396.
29. Y. T. Liu, J. Z. Lu, X. L. Gong, J. J. Liu, B. H. Chen, C. P. Wu and Z. Fang, Formulating compatible non-flammable electrolyte for lithium-ion batteries with ethoxy (pentafluoro) cyclotriphosphazene, *RSC Adv.*, 2024, **14**, 11533-11540.
30. L. H. Zhang, F. Q. Min, Y. Luo, G. J. Dang, H. T. Gu, Q. Y. Dong, M. H. Zhang, L. M. Sheng, Y. B. Shen, L. W. Chen and J. Y. Xie, Practical 4.4 V Li||NCM811 batteries enabled by a thermal stable and HF free carbonate-based electrolyte, *Nano Energy*, 2022, **96**, 107122.
31. K. Chen, D. Zhang, X. Shen, X. Feng, X.-B. Cheng and Y. Wu, Emerging Thermal Safety Characteristics of Large-Capacity Lithium Iron Phosphate Lithium-Ion Batteries, *Adv. Energy Mater.*, 2026, **16**, e03248.
32. Y. Liu, J. Dong, J. Zhou, Y. Guan, Y. Wei, J. Zhao, J. Liang, X. Shi, K. Yan, Y. Lu, N. Li, Y. Su, F. Wu and L. Chen, Interfacial Evolution and Accelerated Aging Mechanism for $LiFePO_4$/Graphite Pouch Batteries Under Multi-Step Indirect Activation, *Nano Micro Lett.*, 2026, **18**, 136.
33. G. Chen, R. Tan, C. Zeng, Y. Li, Z. Zou, H. Wang, C. Ouyang, J. Wan and J. Yang, Developing safe and high-performance lithium-ion batteries: Strategies and approaches, *Prog. Mater. Sci.*, 2025, **154**, 101516.
34. J. Long, J. F. Huang, Y. H. Miao, H. T. Huang, X. C. Chen, J. X. Wu, X. Y. Li and Y. M. Chen, A multi-functional electrolyte additive for fast-charging and flame-retardant lithium-ion batteries, *J. Mater. Chem. A*, 2024, **12**, 17306-17314.
35. Y. T. Liu, Y. L. Zhao, X. L. Gong, Y. Lyu, D. F. Ying, Z. Tang, H. J. Xie, C. P. Wu and B. H. Chen, Enhancing overcharge cycling endurance of lithium-ion batteries via a multifunctional electrolyte, *Mater. Today Adv.*, 2025, **26**, 100586.
36. Y. X. Dong, Z. Q. Zeng, Y. K. Wu, S. P. Wang, C. H. Li, S. Lei, S. J. Cheng and J. Xie, Toward Safe and Cost-Effective $LiFePO_4$ Batteries: A Multifunctional Electrolyte with Flame-Retardant and Interfacial Protection, *ACS Appl. Mater. Interfaces*, 2026, **18**, 16458-16466.
37. K. Huang, Y. Han, Z. Xie, T. Li, Z. Guo, C. Wei, Y. Huang, Y. Liao, J. Wen, Q. Sun, H. Mao, Y. Shen and Y. Huang, Ultrasonic Study of Lithium-Ion Battery Degradation Induced by Transition Metal Dissolution, *ACS Energy Lett.*, 2026, **11**, 3572-3580.
38. H. Li, J. Liu, L. Liu, T. Su, C. Li, S. Ma, Z. Hao, G. Yang, J. Li, T. Ma, F. Wang and J. Ma, Electrolyte Sustaining 4.5 V Li||NCM811 Batteries Cycled at 80°C, *Adv. Energy Mater.*, 2026, e70894. DOI: 10.1002/aenm.70894.
39. X. Luo, Z. Chen, X. Qiu and Y. Qian, Structure and Interfacial-Stable Binder Engineering Enables High-Rate Capability of NCM811 Cathodes at 4.6 V, *Adv. Energy Mater.*, 2026, e70842. DOI: 10.1002/aenm.70842.
40. Y. Liu, J. Dong, Y. Guan, X. Wang, Z. Chen, M. Gao, S. Guo, K. Yan, Y. Lu, M. Wang, N. Li, Y. Su, F. Wu and L. Chen, In Situ 3D Conductive Networks and Interfacial Bonding to Stabilize Oxygen Vacancies for Single-Crystal Ni-Rich Cathodes, *Adv. Mater.*, 2026, **38**, e15106.
41. J. Hao, J. Dong, Y. Guan, Y. Lu, H. Che, Y. Ren, Y. Wang, X. He, Y. Wu, T. Yang, N. Li, Y. Su and L. Chen, Rational design of Li-rich hybrid cathodes with stiff redox-active interstitial networks enabling local environment engineering for reversible oxygen redox, *Energy Storage Mater.*, 2026, **88**, 105121.
42. L. Sun, G. Lu, Q. Han, H. Li, O. Sheng and C. Jin, Additive-induced interfacial chemistry: The key to next-generation lithium metal batteries, *Energy Storage Mater.*, 2025, **82**, 104650.
43. L. Y. Zheng, Z. H. Liu, Y. C. Xie, Y. Wu, T. Deng and X. N. Feng, Enhancing the intrinsic safety of nickel-rich lithium-ion batteries by an ethylene carbonate-free electrolyte with ethoxy(pentafluoro) cyclotriphosphazene additive, *J. Energy Storage*, 2024, **98**, 113165.
44. X. Xin, Q. Yin, Z. Zhao, J. Qi, T. Xu, Z. Li, F. Li, F. Chen, S. Wu and Q.-H. Yang, Wheel-Hub-Inspired Silicon Anodes with Superior Stress Tolerance for High-Energy Lithium-Ion Batteries, *Adv. Energy Mater.*, 2026, **16**, e06650.
45. L. Yang, R. Song, D. Lv, M. Ding, S. Zhang, J. Liu, W. Hu and C. Zhong, Biomass-derived porous hard carbon/silicon anode with superior cycling stability for lithium-ion batteries, *Mater. Today Chem.*, 2026, **51**, 103271.
46. Y. Luo, D. Yang, Z. Chen, L. Wang, B. Xu, G. Zhou and W. Liu, Stress-Dissipating Cocontinuous Carbon–Silicon Microparticles for High-Energy Lithium-Ion Batteries with Low Expansions, *Nano Lett.*, 2025, **25**, 15231-15239.
47. A. Ghaur, F. Pfeiffer, D. Diddens, C. Peschel, I. Dienwiebel, L. L. Du, L. Profanter, M. Weiling, M. Winter, T. Placke, S. Nowak and M. Baghernejad, Molecular-Cling-Effect of Fluoroethylene Carbonate Characterized via Ethoxy(pentafluoro)cyclotriphosphazene on SiO_x/C Anode Materials - A New Perspective for Formerly Sub-Sufficient SEI Forming Additive Compounds, *Small*, 2023, **19**, 2302486.
48. L. T. Dong, L. Q. Deng, Z. F. Wang, Y. Y. Liu, J. Zhan, S. H. Wang, Z. W. Fang, F. F. Guo, C. Liu, H. Liu and H. Chen, A self fire-extinguishing and high rate lithium-fluorinated carbon battery realized by ethoxy (pentafluoro) cyclotriphosphazene electrolyte additive design, *Nano Energy*, 2024, **131**, 110309.
49. Y. Q. Wang, X. Wang, P. Gao, J. C. Jiang and A. C. Huang, Novel composite electrolyte additive for enhancing the thermal and cycling stability of SiO/C anode Li-ion battery, *Process Safety and Environmental Protection*, 2024, **189**, 756-767.

View Article Online DOI: 10.1039/D6SC03275C

View Article Online
DOI: 10.1039/D6SC03275C

Data availability

No primary research results, software or code have been included and no new data were generated or analysed as part of this review.